THE ASTROPHYSICAL JOURNAL, 226:186–202, 1978 November 15

CNO ABUNDANCES AND HYDRODYNAMIC STUDIES OF THE NOVA OUTBURST. V. 1.00 $M_\odot$ MODELS WITH SMALL MASS ENVELOPES*

SUMNER STARRFIELD
Theoretical Division, University of California Los Alamos Scientific Laboratory;
Department of Physics, Arizona State University
JAMES W. TRURAN
Department of Astronomy, University of Illinois
AND
WARREN M. SPARKS
Goddard Space Flight Center, NASA Greenbelt, Maryland
Received 1978 March 28; accepted 1978 May 17

ABSTRACT

We report on an investigation into the consequences of thermonuclear runaways in $10^{-4}\ M_\odot$ accreted hydrogen envelopes on $1.00\ M_\odot$ white dwarfs. These evolutionary sequences predict that from $10^{-5}\ M_\odot$ to $5 \times 10^{-5}\ M_\odot$ will be ejected with speeds from 300 to 3800 km s^{-1} (kinetic energies of 10^{44}–10^{45} ergs). Absolute visual magnitudes as high as -8.1 mag are attained, well within the observed range for fast novae. In addition, the shapes of the theoretical light curves are more reminiscent of an observed fast nova light curve than those in our earlier studies.

The ejected material is strongly enhanced in the products of incomplete CNO burning: the most abundant of the ejected nuclei is ^{13}C, followed by ^{14}N and ^{12}C. The differences from previous studies are attributable to the lower peak temperatures reached in these sequences. These models also produce a large ($\sim$200) overabundance of ^{7}Li, suggesting that novae may represent significant contributors to the galactic enrichment of this nucleus.

We discuss the effects of circumbinary material on the light curve. We suggest that the presence of this gas, the remnant of nonconservative mass transfer, can strongly affect the shape of the light curve around maximum visual magnitude in an actual nova outburst.

We find, as in our earlier work, that these models do not eject their entire accreted envelopes in the earliest stages of the outburst. The residual envelopes quickly evolve to configurations which are hot and bright, representing the probable source for the UV radiation observed in all recent classical novae.

Subject headings: nucleosynthesis — stars: accretion — stars: interiors — stars: novae — stars: white dwarfs

I. INTRODUCTION

In a series of papers, we have investigated thermonuclear runaways (TRs) occurring in hydrogen-rich envelopes on carbon-oxygen white dwarfs and have shown that the behavior of the resulting evolutionary sequences strongly resembles classical fast nova outbursts (cf. Starrfield, Sparks, and Truran 1976; Sparks, Starrfield, and Truran 1977). We have surveyed the effects of variations in the chemical composition, the mass of the white dwarf, and its luminosity, but have held the mass of the hydrogen envelope (M_e) reasonably constant. In our initial studies of the evolution on $1.00\ M_\odot$ white dwarfs, we used $10^{-3}\ M_\odot$ for M_e, basing this value on the hydrostatic study of accretion onto a $0.5\ M_\odot$ white dwarf (Giannone and Weigert 1967), although there was reason to believe that a smaller value might be more appropriate (Starrfield 1971). Recently, however, Taam and Faulkner (1975) and Taam (1978) have considered mass accretion onto $1.00\ M_\odot$ white dwarfs and have shown that an envelope mass as small as $10^{-4}\ M_\odot$ is sufficient to initiate a TR. Similarly, we have performed studies of TRs in hydrogen-rich envelopes of even lower mass and have determined that $5 \times 10^{-5}\ M_\odot$ may be sufficient under some circumstances (Truran *et al.* 1977).

We regard these studies as sufficient justification to survey the evolution with hydrogen envelopes of smaller mass. Specifically, we have adopted $M_e = 10^{-4}\ M_\odot$ as typical of the envelope mass at runaway for $1.00\ M_\odot$ white dwarfs. The characteristics of the resulting evolutionary sequences are sufficiently unlike those of our earlier studies (Starrfield, Sparks, and Truran 1974*a*, hereafter SST) to justify this study. Our light curves are radically different—one sequence actually shows a rounded maximum reminiscent of the light curve of Nova V1500 Cygni 1975. Furthermore, the ejected CNO abundances differ strongly from

* Supported in part by NSF grants AST 73-05271-A02 and AST 76-23190 at Arizona State University and AST 76-22673 at the University of Illinois.

those reported in SST and a much larger fraction of the initial envelope is subsequently ejected due to the delayed energy release from radioactive (positron-unstable) nuclei in the outer regions of the envelope.

In the next section, we discuss several significant changes which have been made to our computer program over the past few years which can affect the evolutionary studies. The methods and approximations used in constructing the initial models for our various evolutionary sequences are described in § III, while § IV contains a comparison with the models published in SST. In §§ V and VI we present the results for models having envelope masses of $10^{-4}\,M_\odot$ and $4 \times 10^{-4}\,M_\odot$, respectively. The critical question concerning the need for and possible source of CNO abundance enhancement is reviewed in § VII. In § VIII, we examine the observational consequences of the current study. A brief summary is presented in the concluding section.

II. METHOD OF COMPUTATION

Our hydrodynamic stellar evolution computer code was first described by Kutter and Sparks (1972); the detailed treatment of the nuclear transformations was outlined by Starrfield *et al.* (1972). The computer code has evolved continuously since that time. Here we describe the three most important changes.

The first of these involves the basic nuclear reaction network. As noted previously (Starrfield *et al.* 1972), we solve a set of differential equations defining the changes in nuclear abundances during a hydrodynamic time step. In our first studies (SST; Starrfield, Sparks and Truran 1974*b*), we computed the abundance changes for each of the 12 nuclei in our network and then used these to determine the rate of nuclear energy generation and neutrino losses (from the positron-decays). This procedure can, under some circumstances, seriously overestimate the neutrino losses. We quickly realized the importance of coupling both the neutrino losses and the energy generation directly to the network; every study of ours since Starrfield, Sparks, and Truran (1974*b*) has used this self-consistent formulation. In order to determine the effect of this change on the evolution, we have recalculated model 9 of SST. As we shall see (§ III), there are only minor changes in the qualitative character of the evolution.

The second major change involves our treatment of the proton-proton reaction sequences. In our earlier work, we used the explicit formulation outlined by Iben (1965). We now treat the proton-proton reaction sequence with a complete reaction network, including the nuclei ^{1}H, ^{3}He, ^{4}He, ^{7}Be, and ^{8}B. Inclusion of nuclei of masses 7 and 8 allows us to determine the abundance of ^{7}Li in the ejected material (Arnould and Nørgaard 1975; Starrfield *et al.* 1978). We have found that these changes can affect the time scale of the outburst (the time to runaway) and the minimum white dwarf luminosity at which a TR will occur.

The third major change involves the treatment of time-dependent, mixing-length convection. We now use a procedure (outlined by Sparks, Starrfield, and Truran 1978) based upon Wood's (1974) formulation, where one iterates on the convective velocity rather than on the convective luminosity. This procedure is generally more stable; furthermore, it utilizes a non-local averaging technique so that it does not suffer from the local instability recently discussed by Kruskal, Schwarzschild, and Härm (1977). The choice of convective treatment does not seem to significantly influence the burst energy generation ejection characteristic of the models described in this paper. It does affect our successful attempt to model the *slow nova* outburst and is described in more detail in that paper (Sparks, Starrfield, and Truran 1978).

III. THE INITIAL MODEL

We begin with the hydrogen envelope in place and in both thermal and hydrostatic equilibrium. We justify this configuration by reference to the hydrostatic studies of accretion onto white dwarfs (Giannone and Weigert 1967; Rose 1968; Redkoborodyi 1972; Taam and Faulkner 1975; Colvin *et al.* 1977; Taam 1978). These authors used rates of infall varying from $10^{-5}\,M_\odot\,\mathrm{yr}^{-1}$ to $10^{-13}\,M_\odot\,\mathrm{yr}^{-1}$, and in all cases found that a TR occurred in the envelope.[1] We can use the results of their studies to determine both the amount of mass that can be accreted in the envelope before a TR occurs and the approximate time scale to the beginning of the TR. In addition, their results show that the amount of mass accreted before the TR occurs is a function of both the mass and the initial luminosity of the white dwarf (Starrfield, Sparks, and Truran 1976). The dependence on mass arises from the fact that, since steeper pressure gradients characterize the more msssive white dwarfs, it takes less mass for the bottom of the accreted layer to reach degenerate densities (Starrfield 1971). The dependence on initial luminosity arises because the temperature at the bottom of the envelope is a function of the luminosity, for low mass accretion rates, and because the time to peak burning is a strong function of this same temperature (Truran *et al.* 1977). For $0.5\,M_\odot$ white dwarfs, the mass of the accreted layer ranges from $6 \times 10^{-4}\,M_\odot$ to $1.3 \times 10^{-3}\,M_\odot$ (Giannone and Weigert 1967); while for $1.0\,M_\odot$ white dwarfs the mass of the accreted layer ranges from $5 \times 10^{-5}\,M_\odot$ to $2 \times 10^{-4}\,M_\odot$ (Taam and Faulkner 1975; Truran *et al.* 1977; Taam 1978).

Since all of the hydrostatic studies produce a TR, we are justified in choosing their values for the envelope mass as starting conditions in our study. We must recognize, of course, that starting with the envelope in place and in equilibrium does not necesarily provide us with a realistic estimate of the time to the peak of the flash. Throughout most of the hydrostatic evolution, the accretion time scale is expected to be shorter than the runaway time scale.

[1] Giannone and Weigert (1967) reported that no TR occurred at a mass accretion rate of $10^{-11}\,M_\odot\,\mathrm{yr}^{-1}$. However, they neglected energy generation for temperatures below 8×10^6 K which invalidates this result (Truran *et al.* 1977).

However, since the hydrostatic studies begin with zero hydrogen in the envelope, they will have fairly long evolution times even at high white dwarf luminosities. We use fairly luminous white dwarfs for convenience only, in order to reduce the evolution times to the flash, since we have already shown that the characteristics of the outburst depend only slightly on the luminosity (SST; Starrfield, Sparks, and Truran 1976).

Finally, we note that the assumed initial compositions for most of the reported models are characterized by high abundances of CNO nuclei relative to solar matter. We have found that it is necessary to increase the abundance of ^{12}C in the envelope quite substantially, in order to produce burst mass ejection. A detailed discussion of this matter is given in § VII.

IV. COMPARISON WITH SST: MODELS WITH $M_e = 10^{-3}\ M_\odot$

In order to establish the effects of the various changes that have been made to the program, we recomputed a model that was virtually identical in initial conditions to model 9 of SST (hereafter SST9). The initial conditions for the new model (model 1) and SST9 are given in Table 1. The small differences in the initial temperature and density at the composition interface (T_{ss}, ρ_{ss}) are caused by the fact that we are now using the Kippenhahn, Weigert, and Hofmeister (1967) degenerate electron equation of state to extend the Los Alamos equation of state tables (Cox 1965, private communication) to higher densities. The slightly higher temperature implies an increase in the initial rate of energy generation (from 3.7×10^6 ergs g^{-1} s^{-1} to 4.5×10^6 ergs g^{-1} s^{-1}) which is responsible for the decrease in the runaway time scale, t_{30} (the time required for the temperature in the shell source to evolve to 30 million degrees). The short time scale is entirely a consequence of our high initial luminosity; if we had chosen to begin the evolution with a lower initial luminosity, we could have increased t_{30} to as much as 10^8 to 10^9 yr (SST; Truran *et al.* 1977).

The early evolution of this model is very similar to the evolution of all models characterized by enhanced CNO abundances that were described in our earlier studies (SST). Once the temperature in the shell source (T_{ss}) reaches about 2×10^7 K, a convective region forms just above it and gradually grows toward the surface. The TR grows exponentially: it takes 1.4 years for T_{ss} to grow to 3×10^7 K, 2.5 days longer to reach 10^8 K, and then another 36 seconds to evolve to a peak temperature of 2.5×10^8 K and a peak ϵ_{nuc} of 1.8×10^{17} ergs g^{-1} s^{-1}. The variation with time of T_{ss} is shown in Figure 1; this should be compared with Figure 8 of SST, which shows the temperature variations for SST9. While the general features are similar, model 1 is marked by the very strong peak at a time of 250 s which is absent in SST9. This sharp peak was not present in the earlier study because we overestimated the energy losses due to the neutrino production from the positron emitters (cf. § II). The temperature rise is rapid enough to produce a shock wave which moves through the envelope and penetrates the surface 1.04 s later (Sparks 1969). The shock accelerates the surface layers to velocities exceeding 5000 km s^{-1}; but since these layers still lie deep within the potential well of the white dwarf, $R_{surf} \sim 10^9$ cm, this velocity is insufficient for ejection. The shock deposits a large amount of energy

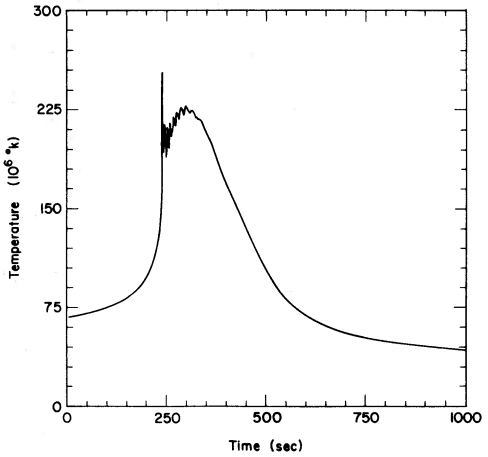

FIG. 1.—The temperature in the deepest hydrogen-rich zone (T_{ss}) as a function of time around the peak of the outburst for Model 1. We begin the plot at a time when the temperature reaches 7×10^7 K. The sharp spike marks the formation of a shock wave.

TABLE 1

THE INITIAL CONDITIONS

PARAMETER	MODEL 1	SST9	2	3	4	5	6	7	8
$L/L_\odot$	1.8−2	1.8−2	1.8−2	1.8−2	1.8−2	1.0−2	1.8−2	1.1−1	1.8−2
Log T_e	4.30	4.30	4.30	4.30	4.30	4.24	4.30	4.54	4.30
Radius (km)	7978	7900	7976	7756	7755	7724	7648	6468	7859
M_e ($M_\odot$)	1.26−3	1.26−3	1.26−3	1.08−4	1.08−4	1.08−4	1.08−4	1.11−4	4.13−4
Log T_{ss} (K)	7.238	7.231	7.232	7.086	7.086	7.035	7.097	7.294	7.178
Log ρ_{ss} (g cm^{-3})	4.147	4.159	4.148	3.386	3.386	3.410	3.519	3.579	3.801
t_{30} (years)	1.40	1.74	1.19	1.15+3	1.0+3	8.8+3	1.4+3	5.4+5	1.6+1
$X(^{12}C)$	0.04	0.04	0.06	0.32	0.45	0.45	0.50	3.2−3	0.12
$X(^{16}O)$	0.04	0.04	7.2−3	7.2−3	7.2−3	7.2−3	7.2−3	3.6−3	7.2−3
ϵ_{nuc} (ergs g^{-1} s^{-1})	4.5+6	3.7+6	5.4+6	5.2+3	5.2+3	7.5+2	2.8+3	3.3+5	5.0+5

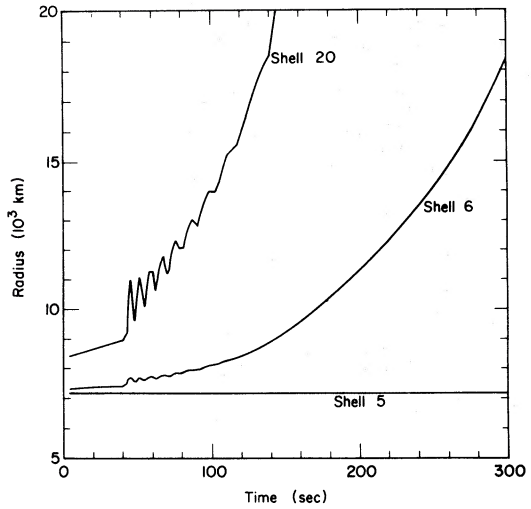

FIG. 2.—The radii of three shells as a function of time for model 1. Shell 5 is just below the composition discontinuity, shell 6 is just above it, and shell 20 is near the top of the convective zone at the time of peak temperature. This plot begins after the temperature has passed 10^8 K.

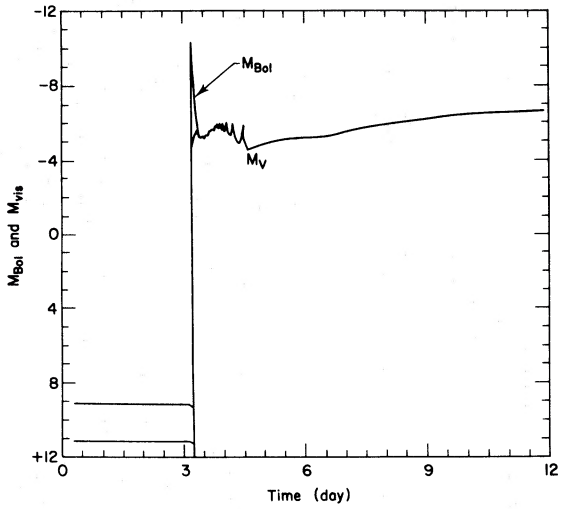

FIG. 3.—The bolometric and visual light curves for model 1. Peak bolometric magnitude occurs when the shock wave penetrates the surface. The bolometric magnitude then drops to +18 mag (see text).

in the surface layers, and the bolometric magnitude climbs to −10.3 mag. However, these layers have also become very hot, $T_e = 1.5 \times 10^6$ K, so that the bolometric correction exceeds 13 mag. These layers are now expanding and cooling very rapidly, and it is impossible for the deeper layers to replenish the energy lost at the surface. Over the next few seconds, M_{Bol} falls precipitously until it has reached $\sim +18$ mag. This lasts for only a few more seconds, and then energy begins to flow into these regions from below and the surface luminosity again begins to rise (cf. Fig. 3).

This stage of the evolution is completely unlike that of SST9, for which no shock wave was produced during the burst energy generation. However, we again find that the initial burst of energy generation has triggered oscillations in the envelope that are ultimately damped as the energy release from radioactive (positron-unstable) nuclei heats the envelope and accelerates the material outward. The oscillations can be seen very clearly in Figure 2, which shows the radii of three shells as a function of time. The heating and cooling of the material in the shell source, as it is compressed and released, is responsible for the oscillations in the temperature that are seen in Figure 1.

Once the influence of the shock has passed, the further evolution of the envelope is very similar to that of SST9. T_{ss} remains at about 2×10^8 K for 100 s, at which point the expansion of the outer layers causes it to drop. It takes another 280 s for the outer layers to reach escape velocity. By this time, T_{ss} has fallen to 1.04×10^8 K and the associated rate of energy generation to 2.7×10^{14} ergs g^{-1} s^{-1}.

It takes this model nearly 5 hours to eject 2×10^{29} g moving with speeds from 360 to 2800 km s^{-1} (total kinetic energy $\sim 8 \times 10^{44}$ ergs). This compares to

TABLE 2

RESULTS OF THE EVOLUTION

PARAMETER	MODEL								
	1	SST9	2	3	4	5	6	7	8
τ_{100}* (days)....	2.5	2.4	2.3	9.4	6.6	7.0	6.6	13.6 yr	5.2
τ_{peak}†.....	36	55	20	55	40	54	34	8.9+3	26
T_{ss} max (K)...	252	219	321	146	146	147	160	176	199
ϵ_{nuc} max (ergs g^{-1} s^{-1})....	1.8+17	3.0+16	1.0+18	2.9+15	4.3+15	4.3+15	6.6+15	1.5+14	3.8+17
M_{ej} (g).....	2+29	3+29	2+28	2+28	7+28	7+28	1+29	NE‡	2+28
V_{min} (km s^{-1})	350	256	335	300	350	339	516	NE	135
V_{max} (km s^{-1})	2800	1900	5738	2200	3200	3300	3822	NE	2868
M_{Bol} (max)....	−9.09	−8.32	−8.94	−9.96	−11.41	−11.38	−12.14	−6.35	−10.10
M_v (max).....	−7.52	−5.91	−6.83	−6.34	−7.57	−7.52	−8.10	+0.1	−6.20
KE (ergs).....	8.5+44	9.8+44	1.5+44	9.4+43	6.5+44	5.9+44	1.3+45	NE	1.1+44

* Time for T_{ss} to evolve from 3×10^7 to 10^8 K.

† Time for T_{ss} to evolve from 10^8 K to peak temperature.

‡ NE = Nothing ejected.

TABLE 3

CNO ABUNDANCES IN THE EJECTA

		MODEL								
ISOTOPE	SOLAR	1	SST9	2	3	4	5	6	7*	8
^{12}C.....	3.39−3	7.4−3	3.5−3	1.2−3	7.3−2	1.3−1	1.3−1	1.6−1	3.6−4	4.1−3
^{13}C.....	4.11−5	5.7−3	9.6−3	1.6−2	1.7−1	2.3−1	2.3−1	2.7−1	1.1−4	2.1−2
^{14}N.....	1.23−3	3.1−2	2.3−2	3.6−2	1.1−1	1.2−1	1.2−1	1.2−1	9.9−3	8.4−2
^{15}N.....	4.82−6	4.5−2	4.2−2	1.8−2	2.0−3	9.8−4	7.8−4	7.1−4	4.4−7	3.6−2
^{16}O.....	8.27−3	8.4−3	2.8−2	6.7−3	7.1−3	7.1−3	7.1−3	3.6−3	2.3−4	6.4−3
^{17}O.....	4.30−6	1.6−2	9.7−3	5.1−4	7.5−5	6.0−5	5.9−5	3.8−5	8.3−8	7.0−4
^{7}Li.....	7.74−9	NA†	NA	2.4−6	1.4−6	1.1−6	NA	1.2−6	4.0−12	6.7−6

* Envelope abundances—nothing ejected.

† NA, not available.

SST9, which ejected 3×10^{29} g (2 more zones) with speeds from 250 to 2000 km s^{-1}. The peak visual magnitudes achieved for the two cases are roughly similar (cf. Table 2), although we were able to follow model 1 (the light curve is shown in Fig. 3) for a longer time as its visual magnitude climbed to −7.5 mag. However, by this time the escaping material has become optically thin, and it is not clear how our diffusion approximation affects the results. The abundances in the ejecta for model 1 and SST9 are presented in Table 3. As neither of these cases was run with the updated *p-p* network, we make no prediction for ^{7}Li.

The remnant envelope contains a major fraction of the initial hydrogen envelope mass, $\sim 2.24 \times 10^{30}$ g (90%). During the outburst it expanded to a radius of 6×10^{11} cm, with velocities exceeding 40 km s^{-1}, before beginning to collapse. At the end of the calculated evolution a few days later, its velocity has fallen to −0.3 km s^{-1} and its radius to 7×10^{10} cm. It has become very hot and luminous ($L \sim L_{\rm Edd}$)—behavior that is characteristic of all of our post-runaway nova models (Sparks, Starrfield, and Truran 1976*a*).

The evolution of the isotopic abundances was also very similar to what we found for SST9. By the time $T_{\rm ss}$ had reached 10^8 K, the convective region extended 1550 km above the shell source (to within 100 km of the surface). A significant fraction of the ^{12}C initially present in the envelope had been converted to ^{13}N and mixed throughout the convective region, and the ^{13}N abundance had increased to 1.74×10^{-2} by mass (all nuclear abundances will be quoted by mass). However, the temperature was still too low for a large number of $^{13}N(p, \gamma)^{14}O$ reactions to have occurred on this time scale, so that $X(^{14}O)$ was only $\sim 10^{-3}$. This changed drastically over the next few seconds as the temperature climbed to maximum. The peak mass fractions of ^{14}O and ^{15}O reached $\sim 2 \times 10^{-2}$. Their abundances declined steadily throughout the rest of the evolution, reaching 9×10^{-3} [$X(^{14}O)$] and 3.3×10^{-2} [$X(^{15}O)$] at the time when the outer layers were just beginning to reach escape velocity. The ^{13}N, ^{14}O, ^{15}O decays were still releasing 10^{10} ergs g^{-1} s^{-1} into the envelope at this stage, as the acceleration of the outer layers continued. These decays gave rise to large overabundances of ^{13}C, ^{14}N, and ^{15}N characteristic of the results of SST.

Our comparison of model 1 and SST9 reveals that the improvements that we have made to the program have changed some of our quantitative results. However, none of the more general conclusions of SST need be amended.

In order to allow a more direct comparison with the models of low envelope mass discussed in the next section, for which the ^{12}C abundance was significantly increased but not that of ^{16}O, we have explored the consequences of just increasing ^{12}C alone for a massive envelope model. Model 2 has exactly the same total envelope mass as Model 1, but we have incorporated 1.5×10^{29} g of ^{12}C into the deepest hydrogen-rich shell while leaving the ^{16}O abundance at the normal (solar) level. This model was calculated after we had added the new proton-proton network; this allowed us to trace the abundance of ^{7}Be and thereby determine the final concentration of ^{7}Li following from $^{7}Be(e^-, \nu)^{7}Li$ on a longer time scale (Starrfield *et al.* 1978). Because the evolution of this model is very similar to that of model 1, we shall comment only briefly on its characteristics. The increased abundance of ^{12}C in model 2 over that in model 1 produces both a higher peak temperature and a steeper temperature rise to maximum ($T_{\rm ss}$ as a function of time is given in Fig. 4). This steep rise again produces a shock wave which is sufficiently energetic to eject 2×10^{26} g with a velocity of 6×10^3 km s^{-1}. The total mass ejected in this case was 2×10^{28} g, nearly a factor of 10 less than was found for model 1. Finally, we find that, excepting ^{17}O, the CNO abundances of the ejected material are reasonably similar to those of model 1.

V. MODELS WITH $M_e = 10^{-4}\ M_\odot$

In this section, we present the main results of this paper: calculations of thermonuclear runaways in envelopes of mass $10^{-4}\ M_\odot$, a factor of 10 less than in our previous studies (SST). As in all our work on the nova outburst, we began by considering the envelope to be of solar composition. The initial ^{12}C concentration was then systematically increased to the point at which mass ejection was found to accompany the

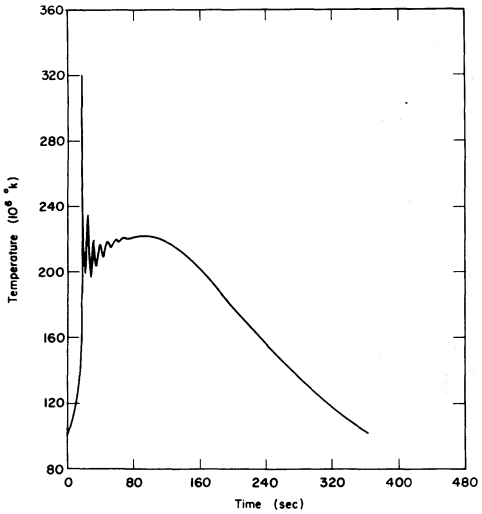

FIG. 4.—The temperature in the deepest hydrogen rich zone (T_{ss}) as a function of time around the peak of the outburst for model 2. The plot is begun just after T_{ss} passes 9×10^7 K. The sharp spike marks the formation of a shock wave which will eject some material.

outburst. The next model to be discussed (model 3) is that with the lowest ^{12}C abundance found sufficient to give rise to mass ejection during the early stages of the outburst. We will report one model of solar composition (model 7) at the end of this section. We note that for all cases discussed below, only ^{12}C was enriched in the envelope—the ^{16}O concentration was left at its solar value. The addition of ^{16}O nuclei can have little influence on these outbursts, as it cannot be burned at the peak temperatures achieved for these models on a hydrodynamic time scale. It might be argued that enrichment of ^{12}C-rich matter is more likely than enrichment of both ^{12}C and ^{16}O (see § VII).

a) Model 3

The initial conditions for this and all subsequent models are given in Table 1. While the luminosity and effective temperature are identical to those for models 1 and 2, the temperature and density at the composition interface are much lower in the presence of the lower envelope mass. In addition, since the hydrogen envelope is smaller, the radius of the dwarf is smaller. For this model, we added 8×10^{28} g of ^{12}C to the deepest hydrogen-rich shells (the average mass fraction of ^{12}C over the envelope is 0.32). This is the same amount of ^{12}C that was added to model 3 of SST (hereafter SST3); the results of the evolution may be compared to that model. One effect of the increased ^{12}C can be seen immediately in the large initial rate of energy generation. A solar mixture at this temperature would be producing energy mostly from the *p-p* chain at a rate of $\sim 1.5 \times 10^2$ ergs g^{-1} s^{-1}.

This model required more than 1000 years to evolve to the peak of the outburst. During the final stages of runaway, it took 9 days to evolve from $T_{ss} = 3 \times 10^7$ K to $T_{ss} = 10^8$ K. While the convective region reached the surface a few days before peak burning, the luminosity only began to rise some hours before the peak of the outburst. The effective temperature is 50,000 K at this time, and only a small fraction of the radiated energy is in the optical. It took this model 55 s to evolve from $T_{ss} = 1.0 \times 10^8$ K to $T_{ss} = 1.39 \times 10^8$ K, which is when peak energy generation occurs [$\epsilon_{nuc}(\max) = 3 \times 10^{15}$ ergs g^{-1} s^{-1}], and then several more seconds to reach peak temperature. Note that the maximum temperature achieved here (1.46×10^8 K) is more than 10^8 degrees lower than was found for model 1. This follows from the fact that, for the lower initial density and temperature in this model, the material is not as degenerate and can begin to expand sooner. In fact, the entire thermonuclear runaway is less violent and events occur much more gradually. No shock is formed in this model; hence no shock ejection of envelope matter occurs.

Mass ejection for this model results entirely from the heating action of the short-lived radioactive CNO isotopes ^{13}N, ^{14}O, and ^{15}O which are convected to the outer regions of the envelope prior to decay. Approximately 1200 s after the peak of the outburst the outermost shells reach a radius of 5×10^{10} cm and a velocity of 10^3 km s^{-1} (escape velocity). The positron-unstable nuclei remain abundant [$X(^{13}N) \sim 4 \times 10^{-2}$], so that the rate of energy release in these shells still exceeds 6×10^{12} ergs g^{-1} s^{-1}. The envelope is continuously accelerated, with the final velocities reaching values in the range from 300 to 2200 km s^{-1} (KE = 9.4×10^{43} ergs).

The light curve for this model is presented in Figure 5; some details of the evolution are collected in Table 2. The ejected mass, kinetic energy, and peak visual

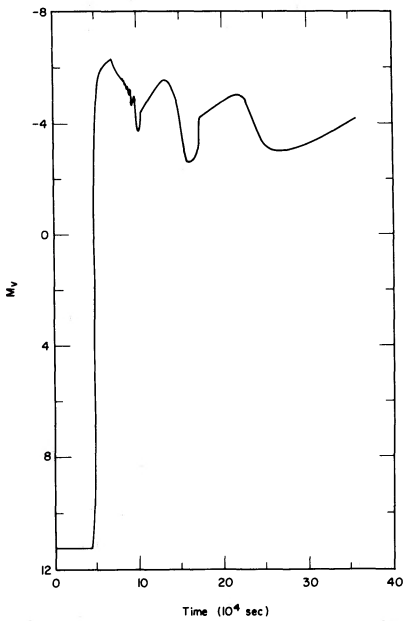

FIG. 5.—The visual light curve for model 3. This model has an envelope mass of $10^{-4}\ M_\odot$, and its shape should be compared to that of model 8 which had an envelope mass of $4 \times 10^{-4}\ M_\odot$ (Fig. 11).

magnitude are somewhat low for a fast nova; as we shall show (model 4), the situation improves with increased ^{12}C enhancements.

Even for this case, however, the final abundances (Table 3) are distinctly different from those of models 1 and 2 and radically change the predictions of SST. As a consequence of the lower peak temperature, ^{13}C rather than ^{15}N is now the most abundant of the ejected nuclei. At 1.5×10^8 K, the $^{13}N(p, \gamma)^{14}O$ rate is much too low for a large number of reactions to occur during the outburst. However, as can be seen from Table 3, enough proton captures occur on ^{13}N to significantly enhance the final abundance of ^{14}N (following the decay of ^{14}O). This decay occurs when it is too cool to burn ^{14}N to ^{15}O; hence the final ^{15}N concentration is only 3×10^{-3}; this is a factor of 10 lower than the value determined for model 1. We also find that the final abundance of ^7Li is 1.5×10^{-6}, an enhancement of nearly 200 over the solar value (Cameron 1973).

b) Models 4 and 5

The initial conditions for model 4 are identical to those of model 3, except that we have increased the ^{12}C concentration in the envelope by about 40%. In fact, roughly 45% of the entire mass of the envelope is now in the form of ^{12}C. The envelope extends 386 km into the dwarf, at which depth the temperature is 12 million degrees and the density is 2400 g cm^{-3}. The initial variation of temperature with radius is shown in Figure 6*a*.

The increased ^{12}C concentration acts to lower the runaway time scale from model 3 by increasing the nuclear energy generation over the entire evolution. (This is not obvious in the initial stages of the outburst, because most of the energy at this state is provided by the proton-proton reaction sequences.) The increased amount of ^{12}C in the envelope similarly reduces the time needed for T_{ss} to evolve from 30 to 100 million degrees by approximately 3 days. The convective region reaches the surface when T_{ss} is about 6×10^7 K, and the intense heating causes these layers to begin expanding at about 8 km s^{-1}. When T_{ss} reaches 10^8 K, the rate of energy generation in the shell source is 5×10^{14} ergs g^{-1} s^{-1}.

It is instructive to note that the mass fraction of ^{14}O at this point has grown to 1.5×10^{-4}; over the next few seconds it will reach and exceed 10^{-3}. Even at these relatively low temperatures, the lifetime for $^{13}N(p, \gamma)^{14}O$ ($\sim$40 s) is less than the ^{13}N positron decay lifetime ($\sim$600 s). The need for a proper treatment of the nuclear physics must be emphasized: the proton capture on ^{13}N cannot be neglected under these conditions.

It takes this model approximately 50 s longer to reach a peak rate of energy generation of 4×10^{15} ergs g^{-1} s^{-1}, and another 0.8 s for the temperature to achieve its maximum value of 1.46×10^8 K. At the time of peak temperature, the rate of energy generation at the surface (from radioactive decays) has reached nearly 3×10^{13} ergs g^{-1} s^{-1}. The temperature distribution at this stage of the evolution is shown in Figure 6*b*. We see from this figure that the outer layers have expanded to over 10^9 cm; this has the effect of reducing the pressure in the layers of the core directly beneath the shell source. Since these layers are not as degenerate as the equivalent material just below the shell source in model 1, they begin to

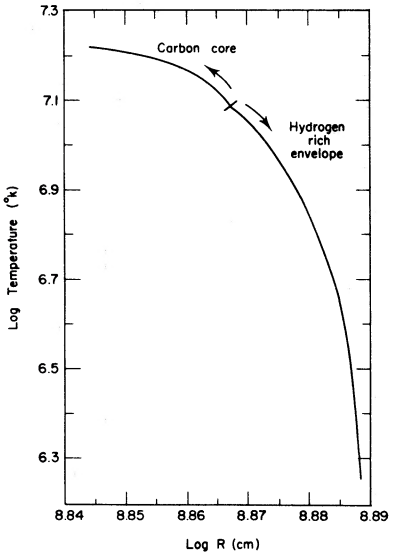

FIG. 6a

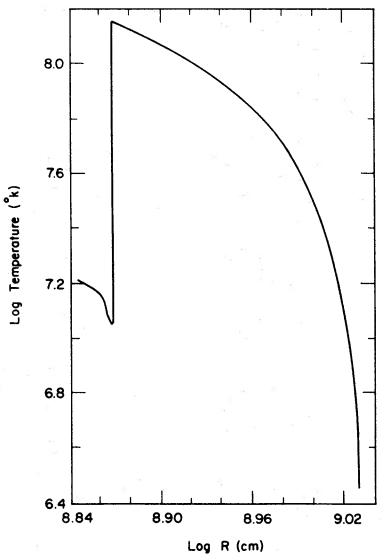

FIG. 6b

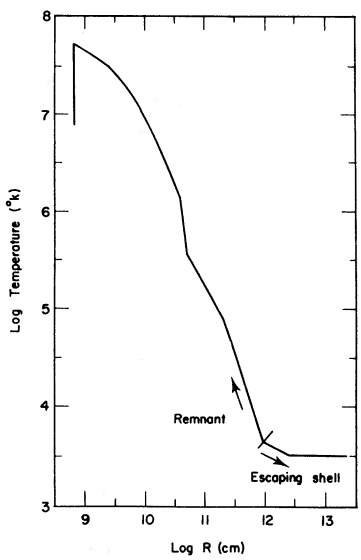

FIG. 6c

FIG. 6.—(*a*) The temperature as a function of radius for model 4 at the beginning of the evolution. (*b*) The temperature as a function of radius for model 4 at the time of peak temperature in the shell source. Note that the edge of the core just below the sharp rise to the peak is convective. (*c*) The temperature as a function of radius for model 4 at the end of the evolution. The escaping material now extends past 10^{13} cm while the hydrostatic remnant reaches to $\sim 3 \times 10^{10}$ cm. Most of the escaping material lies in a shell extending from $\sim 10^{12}$ cm to 3×10^{13} cm.

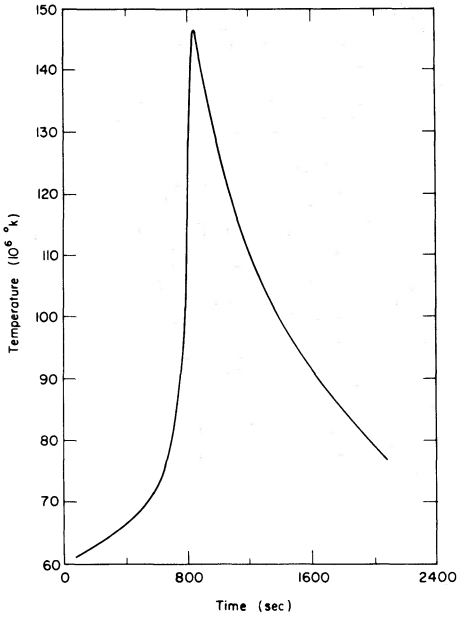

FIG. 7.—The temperature in the shell source (T_{ss}) as a function of time near the peak of the outburst for model 4. Note the very different time scale between Figs. 1, 4, and this figure, and Fig. 10.

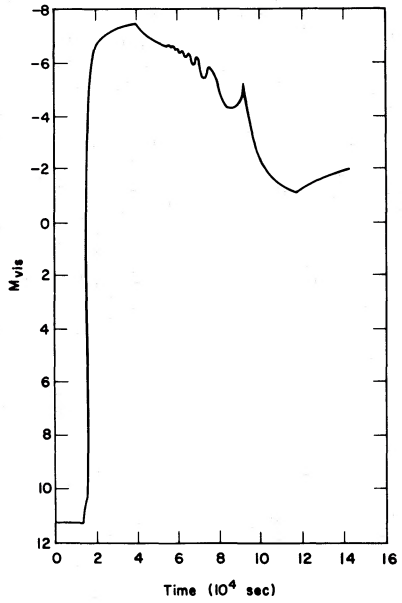

FIG. 8.—The visual light curve for model 4. This model also has an envelope mass of $10^{-4}\ M_\odot$, but the carbon enhancement is greater than in model 3 (cf. Fig. 5).

expand and cool (convection carries the energy produced in the shell source outward). This has the effect of increasing the temperature gradient, and these regions become convective. There is approximately 2×10^{29} g of material involved in the convective region, and the velocities are ~ 2 km s^{-1} and climbing. The top of this region lies about 100 km (roughly 2 pressure scale heights) below the shell source. This phenomenon also occurred in the other small envelope models, in some cases reaching closer to the shell source with even larger convective velocities. It is difficult to assess the effects of overshooting under these conditions; we note, however, that any such overshooting will act to mix fresh ^{12}C nuclei into the envelope when the outburst is near peak temperature. This would certainly have an interesting effect on the nuclear reactions. We regard this as a possible mechanism for enhancing the CNO concentration in the envelope.

The more gradual evolution of this model, as evidence by the variation of temperature with time (Fig. 7), ensures that shock formation does not occur. In addition, there are no oscillations in the envelope. Following peak temperature, the velocity of the surface layers gradually increases until ejection begins. At this time, the positron-unstable isotopes are still abundant and the rate of energy generation exceeds 10^{13} ergs g^{-1} s^{-1}. The heating from their decays is accelerating the material by a factor 1.6 times that of gravity. It takes this model nearly an hour to complete the ejection process; 7×10^{28} g are ejected, moving with speeds from 350 to 3200 km s^{-1}—a kinetic energy of 6×10^{44} ergs (cf. Table 2). This mass represents 32% of the initial envelope, a much larger fraction than we have found in our previous studies.

The visual light curve is given in Figure 8. Here, we note a remarkable difference from SST and models 1 and 2. The light curve shows a rounded peak which lasts for about 1 day. Had it remained at maximum for a bit longer, it would have an optical light curve very reminiscent of Nova V1500 Cygni 1975 (Lockwood and Millis 1976). Model 4 reaches a maximum bolometric magnitude of -11.4 mag (the brightest of our series of low envelope mass models) and a peak visual magnitude of -7.5 mag. This is roughly the peak visual magnitude of a normal fast nova.

The variation of temperature in the envelope at the last time step is shown in Figure 6*c*. The ejected material has a linear variation of velocity with radius (velocity increasing outward). As in all of our studies, we find that a large fraction of the envelope remains on the white dwarf; and although it expands out to $\sim 3 \times 10^{10}$ cm, it quickly returns to hydrostatic equilibrium. The remnant slowly collapses to a radius of $\sim 8 \times 10^9$ cm and becomes convective, luminous, and hot. At the termination of our calculation, the effective temperature has climbed to about 3×10^5 K and the luminosity to $10^5\ L_\odot$. For these conditions, we expect a period of slow mass loss (caused by radiation pressure) which will eject most of the hydrogen material remaining on the white dwarf (Gallagher and Starrfield 1976; Sparks, Starrfield, and Truran 1978). Like the winds observed in O stars, this material should be ejected at high velocities and low densities; its interaction with the higher-density escaping shell could be partially responsible for the very clumpy nature of nova ejecta (McLaughlin 1960; Weaver 1974).

In order to illustrate the overall dependence upon the assumed initial luminosity, we have calculated one further case (model 5) which differs from model 4 only in that its initial luminosity was taken to be $10^{-2} L_\odot$, almost a factor of 2 lower. Its evolution (see Tables 1, 2, and 3) was virtually identical to that of model 4. The notable exception is that the runaway time scale for model 5 (8800 years) is considerably longer than that for model 4 (1200 years). The lower initial luminosity carries with it a lower initial shell temperature and energy generation rate, hence the longer runaway time scale. We interpret the close similarity of the subsequent evolutionary sequences as justification for our choice of more luminous initial configurations.

c) *Model 6*

This is distinguished from previous cases in that the ^{12}C is distributed uniformly throughout the envelope. The initial composition is $X = 0.365$, $Y = 0.134$, and $X(^{12}C) = 0.5$. The increased mean molecular weight throughout the envelope results in a decrease in the radius of the dwarf and increases in the density and the temperature at the composition discontinuity. Nevertheless, the lower ^{12}C abundance in the deepest hydrogen rich shell compared to model 4 ensures that the initial rate of energy generation is smaller and the runaway time scale longer. It takes nearly 7 days for T_{ss} to grow from 3×10^7 K to 10^8 K. During this time the convective region extends farther toward the surface, continually moving into regions with fresh unburned ^{12}C. This model achieves a peak temperature of 1.6×10^8 K and a peak ϵ_{nuc} of 6.6×10^{15} ergs $g^{-1} s^{-1}$; the peak rate of energy generation at the surface reaches 5×10^{13} ergs $g^{-1} s^{-1}$. Shock ejection does not occur in this model; again it is the heating of the outer regions of the envelope by radioactivities that gives rise to ejection of 10^{29} g with a kinetic energy of 10^{45} ergs. The visual light curve for this model is given in Figure 9.

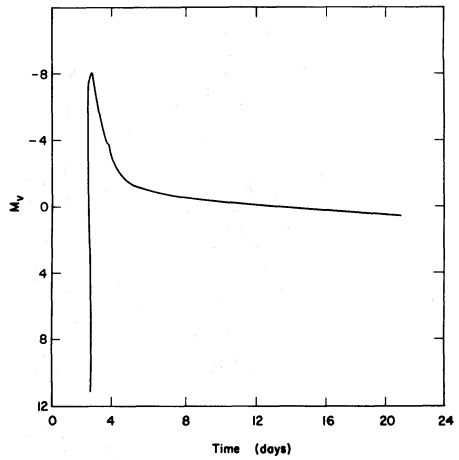

FIG. 9.—The long time behavior of the visual light curve for model 6. For this evolutionary sequence we spread the carbon uniformly through the envelope.

d) *Model 7*

This model was computed as part of an ongoing study of the slow nova outburst (Sparks, Starrfield, and Truran 1978), but its evolutionary behavior also has some implications for the work being reported on this paper. Runaway occurred in an envelope of solar composition on a $1.00 M_\odot$ white dwarf. In this instance, we included the entire white dwarf in the evolution, not just the outer edge of the core and the hydrogen envelope. (We are grateful to Hugh Van Horn for supplying us with this model.) We were able to determine from this study that the flow of energy into the interior does not have any significant effect on the evolution.

The radius of this model is 1200 km smaller than the other models. This is attributable to the fact that our hard-core inner radius was determined by integrating inward from the surface to a radius consistent with the dwarfs calculated by Hamada and Salpeter (1961) while this model includes the entire star and utilizes a different equation of state (Kippenhahn, Weigert, and Hofmeister 1967). This result implies that the models that we have been calling $1.00 M_\odot$ probably represent lower-mass white dwarfs—perhaps as low as $0.9 M_\odot$.

The results for this sequence again demonstrate that models containing a solar abundance of the CNO nuclei do not eject material in the manner of a fast nova outburst. However, the outer layers do reach a radius of 3×10^{10} cm and a luminosity of 2.7×10^4 $L_\odot$, conditions that are certainly sufficient for radiation-pressure–driven mass loss to occur (Sparks, Starrfield, and Truran 1978). As can be seen in Table 3, the abundance results are somewhat different from our previous models since the envelope remains completely convective for a long period; ^{15}N and ^7Li are completely burned out, and the resulting distribution approaches that of steady-state CNO burning, dominated by ^{14}N.

VI. A MODEL WITH $M_e = 4 \times 10^{-4} M_\odot$

In model 8, we study the analog of model 4 with a larger envelope mass. We chose M_e to be slightly larger than the value that Taam and Faulkner (1975) found sufficient to undergo a TR on a $1.00 M_\odot$ white dwarf, in order to evolve a model with initial conditions intermediate between those of our $10^{-3} M_\odot$ and $10^{-4} M_\odot$ studies. We add 10^{29} g of ^{12}C to the envelope, incorporating this into the deepest hydrogen-rich shell; this is equivalent to enhancing the envelope to 12% carbon.

Because of the larger envelope mass (compared to model 4), the conditions at the composition discontinuity are more extreme: the temperature is 1.5×10^7 K, the density is 6.3×10^3 g cm^{-3}, and the initial rate of energy generation is 5×10^5 ergs $g^{-1} s^{-1}$ (cf. Table 1). It now takes 5 days for the shell source to evolve from 3×10^7 K to 10^8 K. Unlike the result for model 4, the convective region has reached to within 55 km of the surface at this time, but

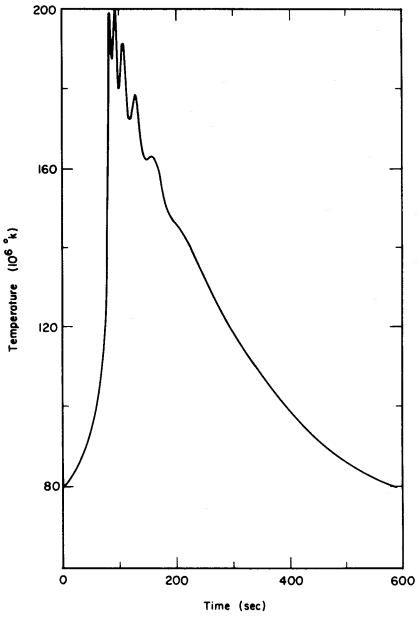

FIG. 10.—The temperature in the shell source (T_{ss}) as a function of time near the peak of the outburst for model 8.

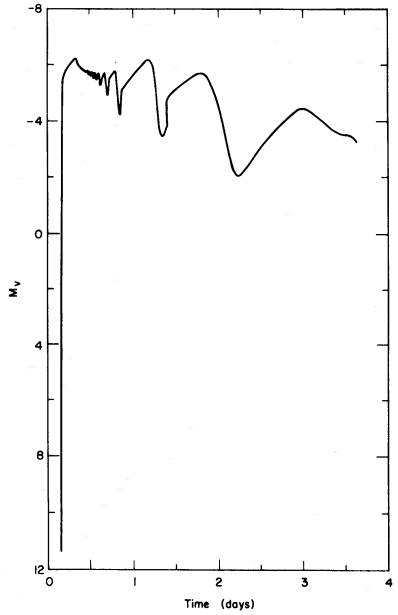

FIG. 11.—The visual light curve for model 8. This model has an envelope mass of $4 \times 10^{-4}\ M_\odot$.

has not actually penetrated the surface. Nevertheless, 55 km is within 2 pressure scale heights of the surface, and any overshooting would allow the energy being produced in the shell source to reach the surface and increase the luminosity of the white dwarf. Energy is being generated in the shell source at a rate of 7×10^{14} ergs g^{-1} s^{-1}; it takes this model only another 26 s to reach a peak burning of 3.8×10^{16} ergs g^{-1} s^{-1} at a temperature of 1.86×10^8 K. The variation of temperature with time for the shell source is shown in Figure 10.

Strong oscillations develop in the envelope, similar to those found for the $10^{-3}\ M_\odot$ envelope models. It would appear that the behavior of T_{ss} with time (Fig. 10) is intermediate between the low envelope mass models and the large envelope mass models. The general shape resembles the $10^{-4}\ M_\odot$ studies, but superposed on this more gradual variation are the strong oscillations characteristic of the $10^{-3}\ M_\odot$ models. Seventeen seconds after peak burning, the outer edge of the core becomes convective. The entire envelope is still oscillating, such that convection will turn on and off in this region over the next few seconds. Nevertheless, at one stage during the evolution the convective velocities reach to nearly 10 km s^{-1} and the top of this convective zone reaches to within 40 km of the bottom of the shell source. Since the pressure scale height in this region is 80 km, the chances seem good that convective overshoot will feed fresh ^{12}C into the shell source. This convective region in the outer edge of the core persists throughout the rest of the evolution; it is, in fact, still present in the hydrostatic remnant after the outburst.

This model ejects 2×10^{28} g moving with speeds from 135 to nearly 2900 km s^{-1}. This is considerably less than was found for model 4 and implies that even more carbon (or ^{16}O) should be added to the envelope to produce results in agreement with the observations. The light curve for this model is given in Figure 11. The light curves of this model and model 3 (Fig. 5) are virtually identical, as are the ejected masses and kinetic energy of the escaping shell. We show the variation of radius with mass at this time in Figure 12. It is apparent that most of the material has been ejected in a shell and that the radius of the hydrostatic remnant extends past the observed Roche lobe radii

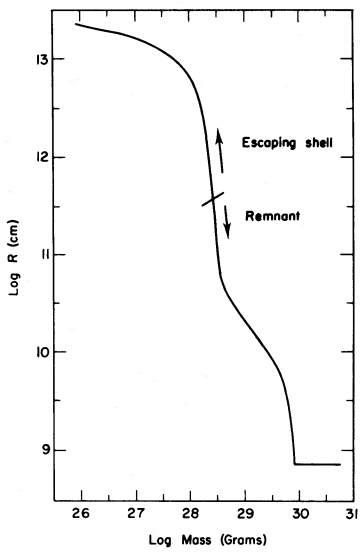

FIG. 12.—The radius of the shell as a function of mass measured *inward from the surface*. Again note that the material has been ejected in a shell which now lies at a distance of $\sim 10^{13}$ cm. The hydrostatic remnant reaches past 10^{11} cm.

of many of the cataclysmic variables. Its outer layers do not start to collapse immediately (as they did in the lower envelope mass models) but grow slowly to a radius of about 6×10^{11} cm and then collapse to 4×10^{11} cm.

The CNO abundances in the ejected shell are given in Table 3. Again, the characteristics of this model lie between the two classes of envelope mass. ^{13}C is more abundant than ^{12}C (similar to the low envelope mass model).

VII. NUCLEAR ENERGETICS, CNO ABUNDANCES, AND NOVAE

We have now demonstrated, both in this paper and in our earlier work, that thermonuclear runaways proceeding in accreted hydrogen-rich envelopes on white dwarfs yield outbursts reproducing many of the observed characteristics of common novae. Throughout our various discussions, we have emphasized both the need for a proper treatment of the nuclear physics and our finding that the characteristics of the outburst can be critically dependent upon the envelope composition. As we shall show below, these are intimately related considerations. In the light of recent observational and theoretical developments, we believe that a clear and concise restatement of our arguments on these matters is appropriate.

In our models, a TR occurs because the base of the hydrogen envelope extends to depths at which the matter is highly degenerate. Following the initiation of nuclear burning in this region, expansion of this material in response to rapid heating is inhibited until temperatures $\sim 10^8$ K, sufficient to lift the degeneracy, are achieved. It follows that, during the final stages of a runaway, nuclear energy generation is provided by hydrogen burning on carbon, nitrogen, and oxygen isotopes. Under normal stellar conditions, the rate of energy generation by these reaction sequences is controlled by the rates of charged-particle thermonuclear reactions. In contrast, high-temperature CNO burning is limited by the rates of the intervening positron-decay reactions. This is particularly important under runaway conditions. For those models described in this paper, peak energy generation is achieved less than 50 s after the runaway temperature reaches 100 million degrees (see Table 2). Because this is less than the critical positron-decay lifetimes, significant cycling cannot accompany CNO burning during the final stages of the runaway.

In the absence of cycling, the instantaneous energy achievable from hydrogen burning on CNO nuclei is greatly reduced. Essentially all that can occur is for each nucleus to capture one proton. The energy release per gram of matter is therefore

$$\epsilon_{\rm TR} \sim 10^{18} \bar{Q} \sum_{\rm CNO} Y \text{ ergs g}^{-1} ,$$

where $\epsilon_{\rm TR}$ represents the energy release in the final rapid stages of the runaway, $\bar{Q}$ is some average energy release per reaction in MeV, and the sum is taken over all $Y = X/A$ for CNO nuclei. For solar matter (Cameron 1973), this gives $\sim 2.7 \times 10^{15}$ ergs g^{-1}. In contrast, the gravitational binding of the envelopes of our current solar mass models is

$$\epsilon_g \sim GM/R \sim 2 \times 10^{17} \text{ ergs g}^{-1} .$$

It is therefore clear that the energy release in the runaway stage alone, assuming an envelope of solar composition, is insufficient to give rise to significant rapid mass ejection.

Nova-like outbursts can nevertheless result under such conditions. Following runaway, significant burning of the available hydrogen fuel can proceed on a longer time scale. The total energy available per gram from complete hydrogen burning is of order $3\text{–}4 \times 10^{18}$ ergs g^{-1}, more than is required to eject a large fraction of the envelope. Radiation pressure driven mass loss can then, for some range of choices of other relevant parameters, give rise to a slow nova outburst (Sparks, Starrfield and Truran 1976*b*, 1978; Prialnik, Shara, and Shaviv 1977, 1978).

We have found, however, that the characteristics of fast nova outbursts cannot be reproduced with the assumption that the envelope matter is of solar composition. The rapid development of the visual light curve and, particularly, the burst ejection of matter at higher velocities both seem to demand a more energetic runaway. It is easy to see how the enrichment of the envelope in carbon can give rise to a more violent event. The maximum energy per gram available through runaway may be written

$$\epsilon_{\rm TR} \sim 2.7 \times 10^{15} (R_{\rm CNO}) \text{ ergs g}^{-1}$$

where $R_{\rm CNO}$ is the ratio of the adopted abundance of these nuclei to their solar system value. Increasing $R_{\rm CNO}$ will increase the energy release through the runaway, hence the peak temperature and energy generation rate achieved in the outburst. It will also increase (by roughly the same factor) the concentrations of the positron-unstable isotopes which, when mixed into the outer regions of the envelope by convection prior to their decay (the convective turnover time is of order 10–100 s), give rise to significant surface heating and expansion. It is this delayed energy release in the outer regions of the envelope at lower gravitational potential which we find greatly encourages mass ejection. We also note that, in one extreme case studied (Starrfield, Truran, and Sparks 1975), the runaway energy exceeded the gravitational binding energy and produced shock ejection of more than 10^{29} g at speeds up to $\sim 90{,}000$ km s^{-1}. While this clearly does not represent a typical nova event, it profoundly illustrates the extreme dependence upon envelope composition.

Two serious questions regarding carbon enrichments of the envelopes remain. First, we note that if envelope composition were the single distinguishing feature, there should exist a correlation between the composition of a nova's ejecta and its speed class. The available observational data do not clarify this situation. In support of our picture, we note that the slow nova HR Del 1967 (Robbins and Sanyal 1978) appears solar in composition, while the extremely fast

nova, Nova Cygni 1975 (Ferland and Shields 1978), shows evidence of large CNO concentrations. However, the slow nova DQ Her (Sneden and Lambert 1975; Williams *et al.* 1978) has been found to contain large overabundances of carbon, nitrogen, and oxygen. Further observational studies are essential if this matter is to be clarified. However, we interpret the increasing body of evidence for enrichment of nova ejecta in CNO nuclei as a general confirmation of our picture.

This leads naturally to questions concerning the mechanism for providing such enrichments. We note that the secondary components of the nova variables are sufficiently close to the main sequence that we do not expect any helium burning to have occurred in the core and penetrated the envelope. Therefore, we must conclude that the white dwarf itself has a carbon-oxygen core. One difficulty with this proposal is that of actually producing a massive carbon-oxygen white dwarf in a close binary system, since it is well known that such an object must be the result of case C mass exchange in which significant mass transfer does not occur until the pre–white-dwarf object has begun burning helium in a shell (cf. Paczyński 1971 and references therein). This is inconsistent with the view that the progenitors of the cataclysmic variables are the W UMa stars. These problems have been considered by a number of investigators and recently reviewed by Gallagher and Starrfield (1978). Webbink (1976) has studied the evolution of the W UMa systems and determined that they have insufficient angular momentum to survive as binaries through the growth of a massive degenerate core in one component; he concludes that these systems cannot evolve into the cataclysmic binaries (however, see also Shu, Lubow, and Anderson 1976). In a similar vein, Ritter (1976) argues that nonconservative mass transfer must be an extremely important part of the evolutionary history of the cataclysmic variables and that it seems quite reasonable that these systems could include a carbon-oxygen white dwarf. We believe that existing observational evidence tends to support this view. The large masses of the dwarf components determined by Robinson (1976), some in excess of a solar mass, are far more easily understood as carbon-oxygen white dwarfs than as pure helium dwarfs.

Given an underlying carbon-oxygen core, the mechanism for envelope enrichment of the white dwarf remains unsettled. Lamb and Van Horn (1975) studied the evolution of a 1.0 $M_\odot$, pure carbon, white dwarf and found that it developed a convective surface layer as it cooled from large effective temperatures. It seemed reasonable to expect that if one of these cool white dwarfs accreted hydrogen it would be mixed through the entire convective region. In fact, Colvin *et al.* (1977) have now found that the accreting hydrogen does penetrate to the bottom of the surface convective zone, producing a hydrogen-rich region with a superenhancement of carbon. Unfortunately, the carbon-enhanced region was limited to that fraction of the star which was originally in the convection zone, and the published model did not reach the degree of enhancement that we have found necessary for a fast nova outburst. We note, however, that a lower-mass white dwarf will have a larger convection zone and should realize a larger carbon enhancement (Fontaine and Van Horn 1976), although ejection becomes more difficult.

Another possible means of envelope enrichment becomes apparent following analysis of the hydrodynamic models discussed in this paper. Specifically, we find that, once the TR is under way, the overlying layers expand and relieve some of the pressure on the outer edge of the core, which responds by expanding and cooling. Just after the temperature peaks in the shell source, the temperature gradient at the boundary of the core becomes adiabatic and the material becomes convective. Although the temperature jump is considerable, the convective velocities reach about 10 km s^{-1} at depths less than a pressure scale height below the shell source. It thus seems possible that convective overshooting could feed carbon and oxygen nuclei into the shell source at the peak of the outburst.

A further mechanism is implied by the results of studies by Durisen (1977) and Kippenhahn and Thomas (1978) of the consequences of accretion onto rotating barytropes. They find that the region between the accreted layer and the core is unstable and that mixing may occur. Since the white dwarfs in the cataclysmic variables must be "spun up" during the accretion process, one might expect different rotational velocities in different systems. Their results then suggest that the rotational velocity of the white dwarf is an important parameter in determining the amount of carbon enhancement in the envelope and, thereby, the strength of the outburst.

In the preceding discussions, we have considered only the possibility of direct mixing between the carbon-oxygen core and the hydrogen envelope. We have thus ignored entirely several potentially important effects which may be associated with the intervening helium zone. Note particularly that the evolution of single stars in the mass range ~ 1–$3\ M_\odot$ (giving rise to carbon-oxygen white dwarf remnants) is characterized by a double shell source configuration and thermal pulses associated with the helium burning shell (Schwarzschild and Härm 1967; Iben 1975 and references therein). The helium region itself will typically contain 10–20% by mass of ^{12}C, and envelope enrichment of ^{12}C up to a factor approximately 10 may ultimately result from convective dredging of shell matter into the envelope (Iben 1976; Iben and Truran 1978). It is therefore possible (begging a host of questions concerning the effects of binary evolution) that the prior evolution of some nova systems has left in its wake a white dwarf with a carbon-enriched hydrogen envelope of very low mass.

This also calls to attention the possibility that some of the eruptions associated with cataclysmic variable systems might be attributable to runaways in the helium shells on carbon-oxygen dwarfs (Webbink 1977, private communication). Growth of the helium zone is a natural consequence of hydrogen burning

proceeding in the overlying envelope. Accretion of hydrogen-rich matter leading to a thermonuclear-runaway in the hydrogen shell, followed by a period of hydrogen burning at high luminosity (a conventional nova model), will certainly increase the mass of the helium zone, as presumably only some fraction less than 1 of the accreted matter will be ejected. It seems possible that, following a sequence of runaways in the hydrogen shell, conditions may develop which are conductive to a helium shell runaway. If such occurs, enrichment of the envelope in helium and particularly carbon can again be realized. We are currently investigating the possible implications of helium thermonuclear runaways for nova-like systems.

There are, it would appear, a variety of mechanisms which might account for carbon-enriched hydrogen envelopes on white dwarfs in nova binary system. On this basis, it seems reasonable to suppose that carbon-enrichment represents one important parameter influencing the characteristics of a nova outburst. The models described in this paper should be viewed in this context. We are simply reporting the results of hydrodynamic evolution for the stated initial conditions. We are not modeling specific events, although we do emphasize the similarities between the characteristics of our calculated explosions and those of the class of fast novae. We note, for example, that parametrization in terms of carbon-enrichment alone implies the existence of a class of outbursts, involving models of normal (solar) envelope compositions, which do not eject matter (e.g., model 6 in this paper). Shara, Prialnik, and Shaviv (1977) have sought to identify such with EUV sources, although detailed comparisons with studied objects do not seem to support this view. We would further expect that the turn-on phase should constitute an observable visual outburst, similar in many respects to common nova outbursts.

VIII. THE OBSERVATIONAL CONSEQUENCES

a) The Light Curves

One of the more important results of this work is our finding that the shapes and amplitudes of the theoretical light curves for models of low envelope mass are in much closer correspondence to the shapes and amplitudes of the observed light curves for the fast novae, than were those of any models that we have previously published. We note specifically that our models show a fast rise to maximum, a rather rounded top, and then either a fast decline or oscillations which gradually grow in period and amplitude. For example, the light curve of model 6 (Fig. 9) might easily be mistaken for that of CP Lac (McLaughlin 1960) or the early stages of V603 Aql (Payne-Gaposchkin 1957) or V1500 Cyg (Lockwood and Millis 1976), if one lengthened the time scale of the theoretical light curves by about a factor of 3. We have also found that the more enhanced of our low envelope mass models become brighter at maximum than any of the models of SST. In fact, model 6 reaches an $M_v(\max) = -8.10$ mag, which is only 0.4 mag fainter than GK Per at maximum and 0.1 mag brighter than the mean absolute magnitude determined from nebular parallaxes (McLaughlin 1960). This is in contrast to models calculated with solar abundances, which never exceed $M_v \approx -6.5$ at maximum (Sparks, Starrfield, and Truran 1978).

The increased visual luminosity at maximum is caused by the increased mass fraction of radioactive nuclei in the ejected material. Our numerical studies indicate that approximately the same *number* of ^{12}C nuclei are required in the envelope for ejection to be achieved, roughly independent of envelope mass (the energy requirements are approximately the same). Because the mass of these envelopes is $10^{-4}\ M_\odot$ instead of $10^{-3}\ M_\odot$, the positron-unstable nuclei and (subsequently) their decay daughters constitute a much larger fraction of the ejected material. This means that radioactive decay will provide much more energy per unit mass of envelope, compared to the models in SST; this drives the ejecta to larger velocities and luminosities.

There is still room for improvement in these light curves. We note both that the theoretical light curves are not as sharply spiked as the observed light curves of the very fastest novae and that the subsequent evolution proceeds much more quickly. On the other hand, our *slow* nova light curve fits HR Del remarkably well (Sparks, Starrfield, and Truran 1978). We propose a possible solution to this problem: the existence of circumbinary material that is not included in our theoretical studies. We have previously proposed that the interaction between the material expanding off the white dwarf and a massive accretion disk was responsible for the oval shapes of the nova nebulae (Sparks and Starrfield 1973). Since that time, the studies of the X-ray binaries have argued against the existence of *massive* accretion disks, and it does not seem possible that a disk with a mass of $10^{-9}\ M_\odot$ or $10^{-10}\ M_\odot$ could influence the motion of an ejected envelope with a mass of 10^{-4} or $10^{-5}\ M_\odot$ (cf. Gallagher and Starrfield 1978). However, it does seem clear that nonconservative mass transfer plays an important role in the evolution of the cataclysmic variables (Webbink 1976; Ritter 1976); this implies that there should be a large ($M \sim 10^{-4}\ M_\odot$) amount of material in the equatorial plane of the binary but outside the L_3 point. If such material is present, then it could provide the interaction that produces the oval shapes of the nebulae.

We can also expect that the presence of the circumbinary material will influence the shape of the observed light curves. This material is moving in a direction roughly perpendicular to the material expanding off the white dwarf; the collision should produce a strong shock which would be very efficient at converting some of the kinetic energy of the expanding material into radiative energy. A point in favor of this argument is that our theoretical velocities are larger than the observed velocities for novae of equivalent maximum visual magnitude. It is possible that the material expanding off of the binary was originally moving at higher speeds, and that its collision with

the material surrounding the binary system reduced its velocity. In this case, the first maximum (called the premaximum halt) would arise from the material expanding off the white dwarf, and the real maximum would arise from radiation of the interaction energy between the ejected shell and the circumbinary shell. For example, $10^{-5}\ M_\odot$ of material (the outer layers of the expanding white dwarf) running into an equal amount of material and losing 10^3 km s^{-1} in velocity over a 1 day period could radiate as much as $10^5\ L_\odot$. The relative heights of these maxima, or absence of premaximum halt, would then depend on the density and distribution of the circumbinary material.

One further discrepancy between our theoretical light curves and the observations involves a recent study of the preoutburst light curves of 12 novae by Robinson (1975), who found that in five of 12 novae the light curve showed a gradual rise for some 1–2 years before the steep rise to maximum. None of our models have shown this behavior. Aside from RR Tel, in which the preoutburst variations have been attributed to the secondary, we assume that the gradual rise is an indication that some of the energy being produced in the shell source is reaching the surface. At present, we do not understand how our treatment of energy transport alone could be responsible for this discrepancy.

b) The Hydrostatic Remnants

The $10^{-4}\ M_\odot$ envelope models presented in this paper eject from 2×10^{28} g to 1×10^{29} g, moving with speeds from 300 km s^{-1} to 3800 km s^{-1} (Table 2). For these cases, the ejecta represent a much larger fraction of the original envelopes than was characteristic of the more massive envelope models (cf. SST); note that, for model 6, over 50% of the initial envelope is ejected. Nevertheless, the behavior of the hydrostatic remnants for the models described in this paper strictly parallels that of our earlier studies. After the initial ejection has occurred, the temperature in the shell source drops to a value in the range 40–50 million degrees, which is dependent upon the envelope mass of the remnant. The outer layers initially expand to about 10^{11} cm and then slowly contract. Over the next few weeks, the effective temperature and luminosity of the remnant slowly increase to values exceeding 10^5 K and $10^4\ L_\odot$ (Sparks, Starrfield, and Truran 1976*a*). At the same time, the entire envelope is becoming convective and completely mixed, which allows the positron-unstable nuclei to again reach the surface. In order to study this phase in detail, we evolved the remnant of model 8 after eliminating the mass zones in the escaping shell.

It takes this model nearly 6 months to become fully convective, over which time the temperature in the shell source slowly declines to 4.8×10^7 K. Because the energy generation at the surface exceeds 7×10^4 ergs g^{-1} s^{-1}, the effective temperature has climbed to 1.39×10^5 K and the luminosity to $4 \times 10^4\ L_\odot$ (very close to $L_{\rm Edd}$). We evolved this model for another 5 years, during which period its surface conditions remained nearly constant, and it burned about 5×10^{-3} (fraction by mass) of the remaining hydrogen. At this rate it will take this model another 1000 years to burn out all of the hydrogen and return to minimum.

It is quite clear that the evolution described in the last paragraph does not agree with the observations of the novae. Even though a hot, bright, constant-luminosity phase has been observed during the outburst of all well studied novae (Gallagher and Starrfield 1976, 1978), it does not last for more than a year or two. For example DQ Her, V603 Aql, HR Del, and RR Pic have certainly returned to minimum (Kraft 1959; Gallagher 1974; Gallagher and Holm 1974); the time scale for the decline must be relatively short, if somewhat variable (Gallagher and Starrfield 1978). It seems that the burning of a large amount of nuclear fuel on the white dwarf to exhaustion cannot be the cause of the turn-off, and we must look to other causes for the decline to minimum. There exist two possibilities that must be considered in any study of the nova phenomena.

The first of these is radiation-pressure–driven mass loss. This is very likely responsible for the slow phase of continuous ejection (SST; Sparks, Starrfield, and Truran 1976*a*; Bath and Shaviv 1976; Bath 1978) and has already been shown to be capable of producing a slow nova outburst (Sparks, Starrfield, and Truran 1976*b*, 1978; Prialnik, Shara, and Shaviv 1977, 1978). We expect this mass loss to occur in the form of a high-velocity, low-density wind. It is possible that this wind is related to the diffuse-enhanced and Orion systems of sharp absorption lines, which appear soon after maximum and slowly separate into sets of lines with large blueshifts with respect to the broad principal emission lines (cf. McLaughlin 1960). It also seems reasonable to expect that the collision of this wind with the ejected shell, which has a higher density and is moving more slowly, will give rise to a Rayleigh-Taylor instability that may explain the clumpy nature of the observed ejecta (McLaughlin 1960; Weaver 1974).

It is also possible that the rapid return to minimum is related to our finding that the radii of the theoretical remnants are, in many cases, larger than the radii of the Roche lobes of many of the old novae. We have discussed this phenomenon elsewhere (SST; Sparks, Starrfield, and Truran 1976*a*); Paczyński (1976) has suggested that considerable mass loss may occur under such circumstances. Our estimates of the rates of mass loss, which can occur during this phase of evolution, suggest that rapid turn-off of the nova requires a small mass envelope. We emphasize that the white dwarf must eject the remnant and return to minimum; otherwise, mass accretion onto its surface will not produce another outburst (Paczyński and Żytkow 1978), whereas Ford (1978) has estimated that each nova binary in M31 must undergo at least 500 outbursts.

As the outer layers are gradually lost and the radius shrinks, the envelope will try to maintain its luminosity (Nariai 1974); this will cause an increase in the effective temperature. While this should occur in every

nova just before burnout, we note that no such behavior has been observed. We conjecture that the constant luminosity and increasing effective temperature of the remnant stimulates a flow of material from the secondary. Some fraction of this flow will be ejected from the system and become part of the mass lost during the outburst. The remainder will flow toward the remnant. This material will act as an extended atmosphere on the white dwarf, dilute the radiation field, and effectively "shut off" the UV source. We would then propose that the UV phase of the nova outburst is ended by a combination of radiation-pressure–driven mass loss from the remnant and an increased flow of mass from the secondary onto the white dwarf. If the dwarf is still hot and luminous, it could eject the newly accreted layer and initiate another phase of mass transfer from the secondary. This phenomenon could be the cause of the repeated bursts of mass ejection observed in some novae.

c) CNO *Nucleosynthesis and the Ejected Abundances*

A very important result of this work is that some specific predictions of SST, concerning the composition of the ejecta, must be modified. These differences arise from the fact that the peak temperatures achieved for the current model of $10^{-4}\ M_\odot$ range from 1.5×10^8 K to 2×10^8 K; in contrast, values approaching 2.5×10^8 K characterize our earlier studies. The lower value for the peak temperature, coupled with the increased initial concentration of ^{12}C required to effect ejection, has a number of interesting effects. (1) At the point of maximum nuclear energy generation, the most abundant of the CNO nuclei are ^{13}N and ^{12}C rather than ^{14}O and ^{15}O. (2) Most of the nuclear energy at this stage arises from the $^{12}C(p,\gamma)^{13}N$ reaction, which produces a very large overabundance of ^{13}N. (3) No significant burning of ^{14}N to ^{15}O or ^{16}O to ^{17}F occurs during the outburst. This means that, following the outburst, when ^{13}N decays to ^{13}C and ^{14}O to ^{14}N, these two decay products plus ^{12}C will be the most abundant CNO isotopes in the ejected shell. This is contrary to our findings in SST where the temperatures reached high enough values to burn a significant amount of ^{14}N and ^{16}O and produce a large overabundance of ^{15}N. (4) Because ^{16}O is not burned during the outburst and the original ^{12}C is converted to ^{13}C and ^{14}N, the ratio of oxygen to carbon plus nitrogen in the ejecta can in principle provide a measure of the initial ratio of oxygen to carbon in the core material that enhanced the envelope. From these data, we may be able to infer something of the prior evolutionary history of the core.

Because the envelope masses studied in this paper are more realistic for a $1.00\ M_\odot$ white dwarf, we expect that our predictions concerning ejected abundances are closer to what should be found in an observed outburst. The fact that ^{13}C is more abundant than ^{12}C disagrees with the studies of CN in DQ Her by Sneden and Lambert (1975). This may be related to the distinction between fast and slow novae. Nevertheless, the recent studies of the abundances in the shell expanding around DQ Her strongly imply overabundances of C, N, and O in this material (Williams *et al.* 1978). Similarly, studies of the early nebular phase of Nova Cygni 1975 reveal strong enrichments in the CNO abundances (Ferland and Shields 1978). These results argue strongly that the enhanced carbon, β^+-decay mechanism has been in operation during the outburst and is indeed the probable cause of the outburst. We add one word of caution concerning determinations of abundances in novae ejecta. It now seems certain that some novae (those which show a deep transition in their light curve) form dust (Gallagher 1977). This dust could well be carbon (Ney and Hatfield 1978). If this is true, then the gas phase abundances in the nova ejecta will underestimate the true carbon abundances in those novae which form dust.

IX. SUMMARY

In this paper we have reported on a new series of investigations into the properties and evolution of the classical fast nova outburst. While we have restricted our study to $1.00\ M_\odot$ white dwarfs (other masses will appear in subsequent papers), we have considered envelope masses ranging from 10^{-4} to $10^{-3}\ M_\odot$. We have emphasized that the evolutionary sequences involving smaller envelope masses produce results that are in better agreement with the observed properties of the novae-light curves, ejected masses, and kinetic energies—than the models described in SST.

Absolute visual magnitudes at maximum of -8.1 mag are attained, well within the observed values for the fast novae. The outburst is accompanied by the ejection of $\sim 10^{-5}$ to $5 \times 10^{-5}\ M_\odot$ into the interstellar medium, moving with speeds from 300 to 3800 km s^{-1} (kinetic energies of 10^{44}–10^{45} erg). While these ejection velocities are somewhat large for a normal fast nova (but not V1500 Cygni 1957), we note that a collision with an accretion disk or circumbinary material could reduce the predicted velocities to values consistent with observations. In fact, we have already seen how the existence of circumbinary material might explain the premaximum halt, the very sharp peak in the light curves of the fastest novae, and the differences in the time scales of the theoretical and observational light curves.

For the models with $M_e = 10^{-4}\ M_\odot$, the degree of degeneracy of the matter at the base of the hydrogen envelope is greatly reduced. The matter can therefore expand more readily in response to the runaway, and a more gradual evolution to lower peak temperatures (compared to cases with $10^{-3}\ M_\odot$) results. With the reduction in peak temperature, it was found necessary to increase the ^{12}C concentration of the envelope to a far greater degree to provide sufficient energy to ensure expansion and mass ejection: the envelope of model 4 has a composition of 40% (by mass) CNO nuclei. The ejected matter is also characterized by this

high degree of enrichment of carbon, nitrogen, and oxygen. The most abundant isotopes predicted by our calculations are ^{13}C, ^{14}N, and ^{12}C. No meaningful prediction concerning ^{16}O is possible since ^{16}O is neither appreciably produced nor consumed by nuclear transformations at the temperatures achieved in our current models. Therefore, its abundance in the ejecta should equal its initial abundance. We have increased only the ^{12}C abundances in these models to provide the energy requirements. The total carbon-plus-nitrogen to oxygen ratio in the ejecta should therefore provide a measure of the initial carbon-to-oxygen ratio in the matter in which the envelope has been enriched.

As part of this study, we evolved two models with an envelope mass of $10^{-3}\ M_\odot$. In both cases the rise to peak temperature is rapid enough to produce a shock wave; this shock is strong enough in one model (model 2) to eject some material when it passes through the surface. In contrast, no shocks were produced in the models with envelope masses of $10^{-4}\ M_\odot$ or $4 \times 10^{-4}\ M_\odot$. This is in disagreement with Sparks (1969), who found that some novae showed evidence that part of the ejected envelope was shock-ejected. Nevertheless, the appearance of shock ejection could arise from the interaction of the material expanding off the white dwarf either with the accretion disk or with circumbinary material.

We have demonstrated that ^7Li production is an important consequence of the nova outburst. Concentrations of ^7Li in excess of 100 times the solar system value may characterize the ejecta. This implies that nova outbursts may represent a major source of ^7Li in the Galaxy (Starrfield *et al.* 1978).

Not all of the material is ejected during the initial outburst; the remaining material quickly returns to hydrostatic equilibrium and evolves to a configuration that is hot and luminous. A long-lived remnant of this nature is inconsistent with observations of nova systems. We expect that this remnant will slowly lose mass either through Roche lobe overflow or a strong stellar wind. Such a wind could be responsible both for accelerating the shell ejected earlier (Arhipova and Mustel 1975) and for causing the clumpiness in the shell through the action of a Rayleigh-Taylor instability.

The range in observed properties of novae is therefore defined by dependences upon such diverse factors as the mass of the white dwarf, the mass transfer rate, the degree of CNO enrichment of the envelope, the rotation rate of the white dwarf, and the amount and distribution of the material which lies just outside the binary.

We would like to express our special thanks to J. Gallagher and R. Webbink for many fruitful discussions with regard to novae. We acknowledge useful discussions with J. Audouze, A. N. Cox, G. Ferland, I. Iben, E. Robinson, G. Shields, P. A. Strittmatter, R. Taam, R. E. Williams, and H. M. Van Horn. We also thank G. Atencio of the Theoretical Division, Los Alamos Scientific Laboratory, for preparing the figures for publication. S. Starrfield would like to thank P. Carruthers and A. N. Cox for the hospitality of the Los Alamos Scientific Laboratory and a generous allotment of computer time. He is also grateful to the Campus Computing Service of Arizona State University for a generous allotment of computer time. S. S. and J. W. T. are grateful to the Aspen Center for Physics for its hospitality in 1975 June and 1976 June.

REFERENCES

Arhipova, V. P., and Mustel, E. R. 1975, in *Proc. IAU Symposium 67, Variable Stars and Stellar Evolution*, ed. V. E. Sherwood and L. Plaut (Dordrecht: Reidel).
Arnould, M., and Nørgaard, H. 1975, *Astr. Ap.*, **42**, 55.
Bath, G. 1978, *M.N.R.A.S.*, in press.
Bath, G., and Shaviv, G. 1976, *M.N.R.A.S.*, **175**, 305.
Cameron, A. G. W. 1973, *Space Sci. Rev.*, **15**, 121.
Colvin, J., Van Horn, H. M., Starrfield, S., and Truran, J. W. 1977, *Ap. J.*, **212**, 791.
Durisen, R. H. 1977, *Ap. J.*, **213**, 145.
Ferland, G., and Shields, G. 1978, *Ap. J.*, **226**, in press.
Fontaine, G., and Van Horn, H. M. 1976, *Ap. J. Suppl.*, **31**, 467.
Ford, H. 1978, *Ap. J.*, **219**, 595.
Gallagher, J. S. 1974, *Bull. AAS*, **6**, 211.
———. 1977, *A.J.*, **82**, 209.
Gallagher, J. S., and Holm, A. V. 1974, *Ap. J. (Letters)*, **189**, L123.
Gallagher, J. S., and Starrfield, S. G. 1976, *M.N.R.A.S.*, **176**, 53.
———. 1978, *Ann. Rev. Astr. Ap.*, **16**, in press.
Giannone, P., and Weigert, A. 1967, *Zs. f. Ap.*, **67**, 41.
Hamada, T., and Salpeter, E. E. 1961, *Ap. J.*, **134**, 683.
Iben, I. 1965, *Ap. J.*, **141**, 1015.
———. 1975, *Ap. J.*, **196**, 525.
———. 1976, *Ap. J.*, **208**, 165.
Iben, I., and Truran, J. W. 1978, *Ap. J.*, **220**, 980.
Kippenhahn, R., and Thomas, H. C. 1978, *Astr. Ap.*, **63**, 265.
Kippenhahn, R., Weigert, A., and Hofmeister, E. 1967, in *Methods of Computational Physics*, Vol. **7**, ed. B. Alder, S. Fernbach, and M. Rotenberg (New York: Academic Press), p. 129.
Kraft, R. P. 1959, *Ap. J.*, **130**, 110.
Kruskal, M., Schwarzschild, M., and Härm, R. 1977, *Ap. J.*, **214**, 498.
Kutter, G. S., and Sparks, W. M. 1972, *Ap. J.*, **175**, 407.
Lamb, D. Q., and Van Horn, H. M. 1975, *Ap. J.*, **200**, 306.
Lockwood, G. W., and Millis, R. L. 1976, *Pub. A.S.P.*, **88**, 235.
McLaughlin, D. B. 1960, in *Stars and Stellar Systems*, Vol. **6**, ed. J. L. Greenstein (Chicago: University of Chicago Press), chap. 17.
Nariai, K. 1974, *Astr. Ap.*, **36**, 231.
Ney, E., and Hatfield, B. F. 1978, *Ap. J. (Letters)*, **219**, L111.
Paczyński, B. 1971, *Ann. Rev. Astr. Ap.*, **9**, 183.
———. 1976, in *Proc. IAU Symposium 73, Structure and Evolution of Close Binary Systems*, ed. P. Eggleton, S. Mitton, and J. Whelan (Dordrecht: Reidel), p. 75.
Paczyński, B., and Żytkow, A. 1978, *Ap. J.*, **222**, 604.
Payne-Gaposchkin, C. 1957, *The Galactic Novae* (reprinted, New York: Dover).
Prialnik, D., Shara, M. M., and Shaviv, G. 1977, in *Novae and Related Stars*, ed. M. Friedjung (Dordrecht: Reidel), p. 220.
———. 1978, *Astr. Ap.*, **62**, 339.
Redkoborodyi, Y. N. 1972, *Astrofizika*, **8**, 261.
Ritter, H. 1976, *M.N.R.A.S.*, **175**, 279.

Robbins, R. R., and Sanyal, A. 1978, *Ap. J.*, **219**, 985.
Robinson, E. L. 1975, *A.J.*, **80**, 515.
———. 1976, *Ann. Rev. Astr. Ap.*, **14**, 119.
Rose, W. K. 1968, *Ap. J.*, **152**, 245.
Schwarzschild, M., and Härm, R. 1967, *Ap. J.*, **150**, 961.
Shara, M. M., Prialnik, D., and Shaviv, G. 1977, *Astr. Ap.*, **61**, 363.
Shu, F. H., Lubow, S. H., and Anderson, L. 1976, *Ap. J.*, **209**, 536.
Sneden, C., and Lambert, D. L. 1975, *M.N.R.A.S.*, **170**, 533.
Sparks, W. M. 1969, *Ap. J.*, **156**, 569.
Sparks, W. M., and Starrfield, S. G. 1973, *M.N.R.A.S.*, **164**, 1 P.
Sparks, W. M., Starrfield, S., and Truran, J. W. 1976*a*, *Ap. J.*, **208**, 819.
———. 1976*b*, *Bull. AAS*, **8**, 321.
———. 1977, in *Novae and Related Stars*, ed. M. Friedjung (Dordrecht: Reidel), p. 291.
———. 1978, *Ap. J.*, **220**, 1063.
Starrfield, S. G. 1971, *M.N.R.A.S.*, **152**, 307.
Starrfield, S., Sparks, W. M., and Truran, J. W. 1974*a*, *Ap. J. Suppl.*, **28**, 247 (SST).
Starrfield, S., Sparks, W. M., and Truran, J. W. 1974*b*, *Ap. J.*, **192**, 647.
———. 1975, *Mém. Roy. Soc. Liège*, 16th Ser., **8**, 413.
———. 1976, in *Structure and Evolution of Close Binary Systems*, ed. P. Eggleton, S. Mitton, and J. Whelan (Dordrecht: Reidel), p. 155.
Starrfield, S., Truran, J. W., and Sparks, W. M. 1975, *Ap. J. (Letters)*, **198**, L113.
Starrfield, S., Truran, J. W., Sparks, W. M., and Arnould, M. 1978, *Ap. J.*, in press.
Starrfield, S., Truran, J. W., Sparks, W. M., and Kutter, G. S. 1972, *Ap. J.*, **176**, 169.
Taam, R. 1978, *Ap. Letters*, **19**, 47.
Taam, R., and Faulkner, J. 1975, *Ap. J.*, **198**, 435.
Truran, J. W., Starrfield, S., Strittmatter, P. A., Wyatt, S. P., and Sparks, W. M. 1977, *Ap. J.*, **211**, 539.
Webbink, R. F. 1976, *Ap. J.*, **209**, 829.
Weaver, H. F. 1974, in *Highlights of Astronomy*, Vol. 3., ed. G. Contopoulos (Dordrecht: Reidel), p. 509.
Williams, R. E., Woolf, N. J., Hege, E. K., Moore, R. L., and Kopriva, D. A. 1978, *Ap. J.*, in press.
Wood, P. R. 1974, *Ap. J.*, **190**, 609.

WARREN M. SPARKS: Laboratory for Astronomy and Solar Physics, Code 681 Goddard Space Flight Center, Greenbelt, MD 20771

SUMNER STARRFIELD: Steward Observatory, University of Arizona, Tucson, AZ 85721

JAMES W. TRURAN: Department of Astronomy, University of Illinois, Urbana, IL 61801